# The Folding Kinetics and Thermodynamics of the Fyn-SH3 Domain†

Kevin W. Plaxco,‡,§,|| J. Iñaki Guijarro,‡,§ Craig J. Morton,§,⊥,# Maureen Pitkeathly,‡ Iain D. Campbell,⊥ and Christopher M. Dobson*,‡

*Oxford Centre for Molecular Sciences, New Chemistry Laboratory, and Department of Biochemistry, University of Oxford, South Parks Road, Oxford OX1 3QT, England*

*Received August 21, 1997; Revised Manuscript Received October 27, 1997*

ABSTRACT: The equilibrium unfolding and the kinetic folding and unfolding of the 67 residue Fyn-SH3 domain have been investigated. Equilibrium unfolding experiments indicate that, despite the lack of both disulfide bonds and prosthetic groups, Fyn-SH3 is relatively stable with a free energy of folding of −6.0 ± 0.6 kcal mol$^{-1}$ at 20 °C. Kinetic experiments indicate that the domain refolds in a rapid two-state manner without significant population of intermediates ($k$ = 94.3 s$^{-1}$ in $H_2O$ at 20 °C). Despite the presence of two proline residues, the refolding of the domain is monophasic, and no significant proline isomerization-like refolding phase is observed. This can be attributed to an extremely low level of the incorrect (*cis*) isomer of the structurally important Pro134 residue in the protein denatured in 8 M guanidine hydrochloride. Analysis of the temperature and guanidine hydrochloride dependence of the folding rate suggests that the folding transition state of this protein is relatively well organized. A comparison with the refolding kinetics and thermodynamics of other homologous SH3 domains indicates that these exhibit an equivalent degree of transition state organization. This potentially arises from conservation of key features of the transition state conformation despite sometimes relatively low overall sequence identity. Such a comparison further suggests that relative thermodynamic stability is an important factor in determining the relative folding rates of natural proteins with a common fold, but that specific details of the amino acid sequence can also play a significant role in individual cases.

Small, monomeric, single-domain proteins lacking kinetically complicating factors such as disulfide bonds, prosthetic groups, or native *cis*-proline residues are relatively simple systems for the study of protein folding. Comparison of the refolding of members of a homologous family of such kinetically simple proteins provides an opportunity to study the relative importance of various equilibrium properties in defining folding rates in the absence of potentially complicating factors such as significantly differing topologies or structures. With this aim, we have characterized the refolding kinetics of the src homology 3 domain of human Fyn tyrosine kinase (Fyn-SH3).[1]

The SH3 domain is a small (∼60 residue) protein module found in a large number of multidomain proteins, primarily those involved in cellular signaling (*1*). This module has been well characterized by both NMR and X-ray techniques and is a small $\beta$-barrel composed of two perpendicular $\beta$-sheets, lacking disulfide bonds and *cis*-proline residues. The SH3 domain provides an excellent system for studying the kinetics and thermodynamics of protein refolding due to this structural simplicity. Detailed characterizations of the folding kinetics of the related spectrin (*2*), src (*3*, *4*) and PI3 SH3 (PI3-SH3, ref *5*) domains have already been carried out. The preliminary investigation of refolding of the drk SH3 domain has also been reported (*6*). The solution structures of the SH3 domain from human Fyn both alone (*7*) and complexed with poly-proline peptide ligands (*7*, *8*) have recently been described. We present here the kinetics and thermodynamics of the refolding of the Fyn-SH3 domain and discuss the implications of these data for the structure of the folding transition state and the determinants of protein folding kinetics.

## MATERIALS AND METHODS

Recombinant human Fyn-SH3 was expressed as a glutathione *S*-transferase fusion protein in *E. coli* and purified as described previously (*7*). The construct used consisted of the 67 structured residues of the domain, an amino-terminal 2 residue extension (GS) (*7*), and a carboxy-terminal 6 residue tail (EFIVTD). Pure Fyn-SH3 was exchanged into 20 mM $NH_4HCO_3$ on a DG-10 desalting column (BioRad)

† The Oxford Centre for Molecular Sciences is supported by the U.K. Biotechnology and Biological Sciences Research Council, the Engineering and Physical Sciences Research Council, and the Medical Research Council. This work was also supported in part by the Wellcome Trust (I.D.C.), an International Research Scholars award from the Howard Hughes Medical Institute (C.M.D.) and the European Commission (C.M.D. and J.I.G.).

* To whom correspondence should be addressed. E-mail: chris.dobson@chem.ox.ac.uk.

‡ New Chemistry Laboratory.

§ K.W.P., J.I.G., and C.J.M. contributed equally to this work.

|| Present address: Department of Biochemistry, University of Washington, Seattle, WA 98195.

⊥ Department of Biochemistry.

# Present address: Department of Chemistry, University of Melbourne, Parkville 3052, Australia.

[1] Abbreviations: Fyn-SH3, SH3 domain of human Fyn tyrosine kinase; GuHCl, guanidine hydrochloride; HSQC, heteronuclear single quantum correlation experiment; PI3, phosphatidylinositol 3′-kinase; PI3-SH3, SH3 domain of the p85α subunit of bovine phosphatidylinositol 3′-kinase.

S0006-2960(97)02075-8 CCC: $15.00 
Published on Web 02/05/1998

and lyophilized to produce buffer-free material for folding studies.

Synthetic peptides were produced on an Applied Biosystems automated peptide synthesizer using Fmoc chemistry. Fmoc-[$^{13}$C]proline was produced by reaction of uniformly labeled [$^{13}$C]proline (CK gas products) with Fmoc-succinimide (NovaBiochem). The [$^{13}$C]proline was dissolved in 6% $Na_2CO_3$ at 0 °C, and 1.1 equiv of Fmoc-succinimide in the minimum volume of DMF was added. After mixing, the reaction mixture was left for 3 h at room temperature with constant stirring. The crude product was washed with diethyl ether, and then acidified with citric acid to a final pH value of 3. This solution was extracted with diethyl ether and the material analyzed for purity and composition by HPLC, thin-layer chromatography and mass spectrometry. Analysis indicated that the extracted material was a single species with the expected mass for the Fmoc-proline, and consequently the material was lyophilized and used without further purification.

After cleavage from the support, all peptides were purified by RP-HPLC on a Beckman System Gold HPLC using either a Brownlee 4.6 × 30 mm C8 reverse phase column (ABI) for analytical runs or a Vydac 10 × 250 mm column for preparative work. Analytical run fractions containing peptide were collected manually and lyophilized for analysis by mass spectrometry. Fractions containing peptide from preparative runs were collected manually, pooled, and lyophilized.

Equilibrium unfolding experiments were conducted on recombinant Fyn-SH3 samples (0.1 mg/mL) equilibrated with various concentrations of guanidine hydrochloride (GuHCl) for at least 45 min on a Perkin-Elmer LS 50B fluorimeter thermostated to 20.0 ± 0.5 °C. Sample excitation was at 280 ± 1.25 nm, with emission monitored at 340 ± 1.25 nm. In all experiments, final GuHCl concentrations were determined by refractometry (*9*). Thermodynamic parameters were calculated by fitting the equilibrium data to the equations describing a two-state folding reaction (see ref *10*) using the nonlinear least-squares fitting algorithm in KaleidaGraph (Albeck Software, Reading, PA).

The refolding of Fyn-SH3 was characterized using an SX17-MV stopped-flow fluorimeter (Applied Photophysics) equipped with a Grant LTD6G water bath thermostated to ±0.1 °C. Excitation was at 280 ± 4 nm, with detection above 320 nm by use of the appropriate cut off filter. Kinetic data were obtained by diluting Fyn-SH3 (0.19 mM) in 8.0 M GuHCl, 20 mM Tris-HCl, pH 7.2, 11-fold with 20 mM Tris-HCl, pH 7.2 (Tris). Kinetics of the recovery of peptide binding were followed by including 0.07 mM of a synthetic SH3 ligand peptide (PPRPLPVAPPGSSKT) in the refolding buffer and subtracting the intrinsic fluorescence change from that observed in the presence of peptide. [Peptide binding occurs at a rate of $>1000$ s$^{-1}$, and increases the solvent shielding of the binding cleft tryptophan (*8*), thus producing a large and effectively instantaneous change in net fluorescence]. The GuHCl concentration dependence of Fyn-SH3 refolding was analyzed by monitoring the recovery of native fluorescence as Fyn-SH3 in Tris containing 8 M GuHCl was diluted 11-fold into Tris containing the appropriate amount of GuHCl. The temperature dependence of Fyn-SH3 refolding was followed by measuring the kinetics of refolding at temperatures between 6 and 75 °C after allowing the refolding buffer, the denatured Fyn-SH3, and the fluorimeter cell to equilibrate at each temperature for at least 15 min. The native Fyn-SH3 signal was determined by diluting native Fyn-SH3 in Tris with Tris containing 0.8 M GuHCl (final GuHCl concentration 0.727 M). Unfolding experiments were conducted using either manual mixing on the Perkin-Elmer fluorimeter (for slowly unfolding samples) or the Applied Photophysics stopped-flow fluorimeter (for rapidly folding samples). The final protein concentration was 0.1 mg/mL for the manual mixing and 0.3 mg/mL for the stopped-flow fluorimeter. All other conditions were as described above. Reported values and confidence levels represent the average and standard deviation of 10 measurements (intrinsic fluorescence and peptide binding), fitted values and estimated fitting errors (equilibrium unfolding, temperature dependence, and intrinsic $k_{f-H2O}$, $k_{u-H2O}$, $m^{\ddagger}_{f}$ and $m^{\ddagger}_{u}$), or the average and standard deviation of several peak volume ratios (proline *cis*−*trans* ratios). Control experiments with native protein indicated that small variations in signal intensity due to lamp drift and sample diffusion would prevent detection of small amplitude phases ($<2\%$) with rates of $<0.02$ s$^{-1}$ or intermediate amplitude ($\sim 5\%$) with much slower rates. Data were analyzed using the software supplied with the fluorimeter or the nonlinear least-squares fitting algorithm in KaleidaGraph.

Kinetic NMR measurements were conducted using a pneumatic mixer as previously described (*11*). Fyn-SH3 (final concentration 0.2 mM) in 8.0 M $^2$H−GuHCl was diluted 11-fold in 50 mM sodium phosphate buffer, p$^2$H 7.2 (uncorrected meter reading), in $^2H_2O$ at 20 °C to initiate the refolding of the protein. Experiments were conducted at a proton frequency of 500.1 MHz using a home-built spectrometer based on an Oxford Instruments 11.4 T magnet and a GE-1280 computer. A series of one-dimensional $^1$H spectra was recorded after diluting the protein in the refolding buffer. The delay between each transient was 1 s, and two transients were accumulated. The resulting delay between two spectra is thus 2 s. NMR data were analyzed using the Felix software package (Biosym) on a SGI Indigo computer.

$^1$H−$^{15}$N and $^1$H−$^{13}$C HSQC spectra (*12, 13*) were recorded respectively on $^{15}$N- and $^{15}$N−$^{13}$C-labeled Fyn-SH3 (2 mM) in Tris and in Tris containing 8.0 M GuHCl (prepared with 5% $^2H_2O$). Spectra were recorded at 20 °C at a $^1$H resonant frequency of 500.1 MHz. The *cis*−*trans* proline isomer ratio in the denatured protein can in principle be determined from the ratios of the C$\alpha$H, C$\beta$H, and C$\delta$H *cis* and *trans* peak volumes. However, as these peaks were not well resolved in the denatured protein spectra, $^1$H−$^{13}$C HSQC spectra were also acquired on a specifically labeled synthetic Fyn-SH3 fragment consisting of the 40 carboxy-terminal residues of Fyn-SH3 with a uniformly labeled $^{13}$C-proline at residue 134. Spectra of this material were recorded at a concentration of 2 mM in Tris containing 8.0 M GuHCl and 5% $^2H_2O$. For the synthetic pentapeptide YIPSN dissolved in Tris containing 8.0 M GuHCl (5% $^2H_2O$), the *cis*−*trans* proline isomer ratio was assessed using a one-dimensional $^1$H spectrum. Assignment of *cis*−*trans* signals and the *cis*−*trans* ratio was confirmed using a natural abundance $^1$H−$^{13}$C HSQC spectrum (*12, 13*).

Amino acid sequence alignment and pairwise identity calculations were performed for the SH3 domains from Fyn, src, spectrin, PI3, and drk using the program AMPS (*14*) at the EMBL server.

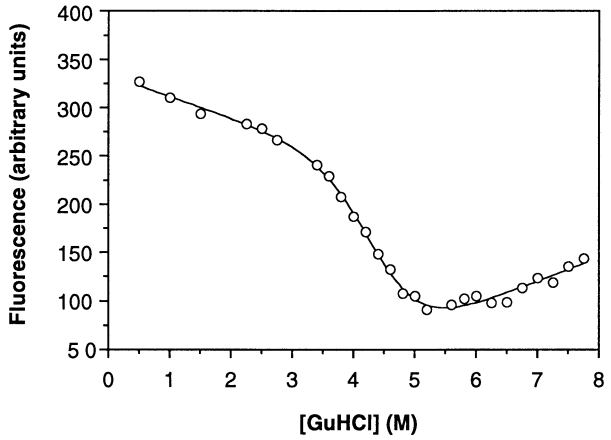


FIGURE 1: Equilibrium denaturation of Fyn-SH3 by GuHCl (20 °C) is well fitted by the equations describing a two-state transition and indicates that the domain is relatively stable ($\Delta G_{H_2O} = -6.0 \pm 0.6$ kcal mol$^{-1}$). The derived $m_{eq}$ value, $1.36 \pm 0.13$ kcal mol$^{-1}$ M$^{-1}$, is very similar to that obtained for other small, globular proteins (*17*).

## RESULTS AND DISCUSSION

Data from the equilibrium chemical denaturation of Fyn-SH3 are well fitted by the equations describing a two-state unfolding transition (*10*) with a free energy of folding ($\Delta G_{H_2O}$) of $-6.0 \pm 0.6$ kcal mol$^{-1}$ (Figure 1). This is relatively high for a small protein lacking disulfide bonds although some other proteins of similar size such as ubiquitin (*15*) and chymotrypsin inhibitor 2 (*16*) display similar stabilities. Compared to other SH3 domains, Fyn-SH3 is very stable. Indeed, the free energies of folding of the structurally related src, spectrin, PI3, and drk SH3 domains are only $-4.1$, $-3.8$, $-3.4$, and $\sim 0$ kcal mol$^{-1}$, respectively (*4*, *10*, *5*, *6*). As SH3 domains display a highly conserved core structure but a relatively low sequence identity, the differences responsible for the higher stability of Fyn-SH3 may be very subtle and remain unclear. No significant intermediates are observed during the equilibrium unfolding of the domain, although a substantial dependence of the fluorescence of the native and denatured states on the concentration of the denaturant GuHCl is observed. The derived GuHCl sensitivity ($m_{eq}$) is $1.36 \pm 0.13$ kcal mol$^{-1}$ M$^{-1}$. The parameter $m_{eq}$ reflects the effect of GuHCl on the relative free energy of the folded state and is thought to parallel the change in solvent-accessible surface area during folding. The value of $m_{eq}$ obtained for Fyn-SH3 compares well with the values derived for other small, single-domain proteins of similar size (*17*).

The refolding kinetics of Fyn-SH3 from 8 M GuHCl are effectively identical whether probed by intrinsic fluorescence or by the recovery of peptide binding activity. The native fluorescence of the two tryptophan residues of the protein, which reflects details of the packing of the hydrophobic core, is recovered with a rate of $25.6 \pm 1.2$ s$^{-1}$ in 0.727 M GuHCl. This refolding is well described (residual amplitudes <3%) by a single-exponential rate equation (Figure 2A) with no significant improvement in the quality of fit (as monitored by residual amplitudes or serial correlation of the residuals) from higher order fits (data not shown). No burst phase event is evident in the intrinsic fluorescence as the single-exponential fit extrapolates at time zero to the expected value for the fluorescence of the unfolded protein in the refolding

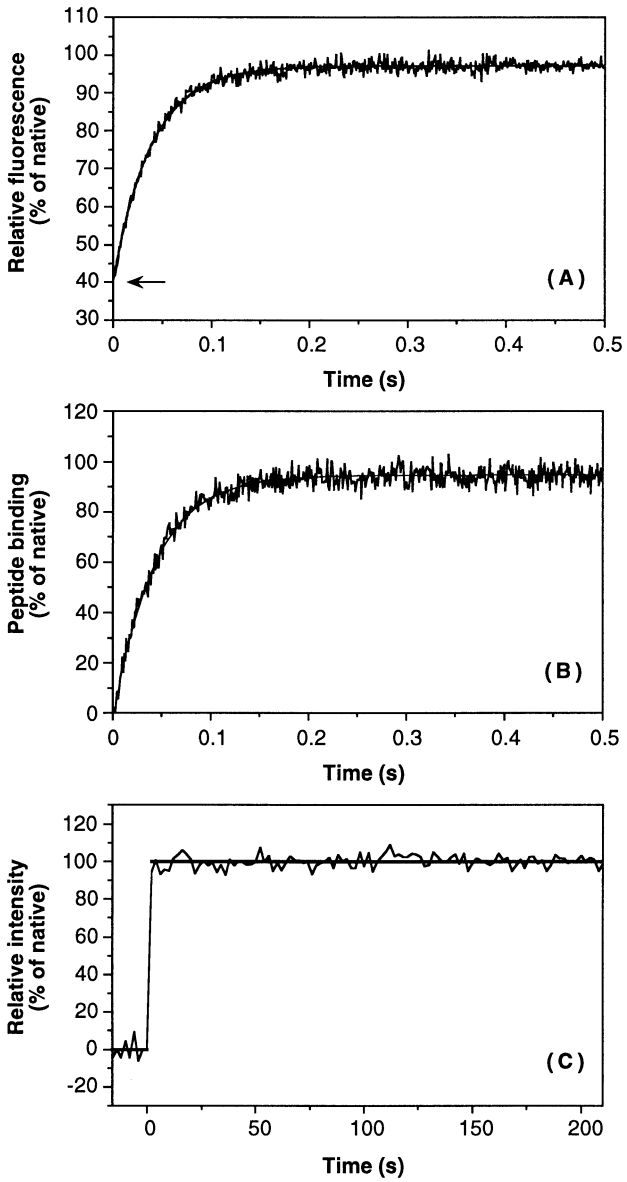


FIGURE 2: Kinetics of refolding of Fyn-SH3 are concerted. Native levels of both intrinsic fluorescence ($97 \pm 3\%$) (A) and peptide binding activity ($95 \pm 6\%$) (B) are recovered with effectively identical kinetics ($25.6 \pm 1.2$ and $23.7 \pm 2.0$ s$^{-1}$, respectively, in 0.727 M GuHCl at 20 °C). Consistent with this observation, the native NMR signal intensity ($95 \pm 8\%$) is recovered within the 2 s dead time of kinetic NMR measurements (C), indicating that a native core geometry is recovered within that time frame. The expected fluorescence of the unfolded protein in the refolding buffer (40%) is indicated in (A) by an arrow. It was calculated by linear extrapolation of the fluorescence of denatured Fyn-SH3 at high GuHCl concentrations.

buffer. The kinetics of the recovery of peptide binding under identical conditions (Figure 2B) are $23.7 \pm 2.0$ s$^{-1}$. That both the core packing geometry and active site tertiary structure are recovered with identical kinetics suggests that Fyn-SH3 folds in a concerted, two-state reaction. Kinetic NMR experiments (*11*), while exhibiting significantly poorer time resolution, are in agreement with this observation since the spectrum acquired $\sim 2$ s after the initiation of refolding is that of the native protein (Figure 2C).

Refolding of the Fyn-SH3 domain as measured by the recovery of native tryptophan fluorescence occurs with an extrapolated intrinsic rate (the folding rate in the absence of

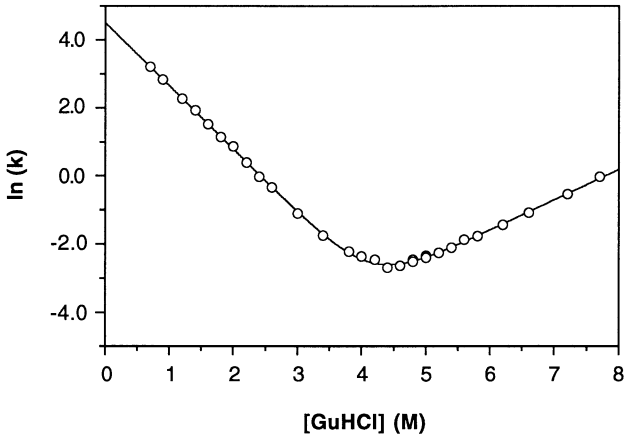


FIGURE 3: Dependence of the kinetics of unfolding and refolding of Fyn-SH3 on GuHCl concentration. The intrinsic folding rate of Fyn-SH3 (the extrapolated rate in $H_2O$, $k_{f-H_2O}$) is 94.3 ± 2.7 $s^{-1}$. The plot of ln ($k$) versus [GuHCl] is linear in the regions away from the folding/unfolding transition. This indicates that the refolding of the domain does not proceed through stable kinetic intermediates (*16*). The slopes of these curves are a measure of the $m^{\ddagger}$ values of the folding and unfolding transition states (*16*). In particular, the ratio $\alpha = m^{\ddagger}_f/(m^{\ddagger}_u - m^{\ddagger}_f)$ is thought to reflect the relative solvent-accessible surface area of the folding transition state. The value of α obtained for Fyn-SH3, 0.68, is very similar to values obtained for both the spectrin (0.69, ref *37*) and src SH3 domains (0.69, ref *3*) and slightly higher than the value determined for PI3-SH3 (0.60, ref *5*). This suggests that all four proteins fold via similar transition state conformations though the PI3-SH3 domain transition state may be slightly less well organized.

denaturant) of 94.3 ± 2.7 $s^{-1}$ (Figure 3). The unfolding rate is relatively slow ($k_{u-H_2O} = 9.9 \times 10^{-4} \pm 1.4 \times 10^{-4}$ $s^{-1}$). Several lines of evidence indicate that the refolding of the domain follows a two-state mechanism lacking significant kinetic intermediates. A plot of ln($k$) versus guanidine hydrochloride concentration is linear away from the folding/unfolding transition region ($r^2 = 0.999$ for both folding and unfolding). Equilibrium parameters ($\Delta G_{H_2O}$ and $m_{eq}$) derived from fitting kinetic data over a broad range of denaturant concentrations to a two-state model are consistent with the equivalent parameters obtained from equilibrium experiments. Indeed, as derived from kinetics (see ref *16*), $\Delta G_{H_2O}$ is −6.68 ± 0.01 kcal $mol^{-1}$, which is within the confidence limits of the value obtained from equilibrium unfolding, and $m_{eq}$, calculated from $m^{\ddagger}_f$ and $m^{\ddagger}_u$ values of −1.09 ± 0.01 and 0.52 ± 0.01 kcal $mol^{-1}$ $M^{-1}$, respectively (Figure 3), is 1.61 ± 0.02 kcal $mol^{-1}$ $M^{-1}$, which is relatively close to the 1.36 ± 0.13 kcal $mol^{-1}$ determined from equilibrium studies. These results suggest that no stable folding or unfolding intermediates are significantly populated during folding (*16*) and are strong evidence that the refolding of the Fyn-SH3 domain is well described as a two-state process.

The native Fyn-SH3 domain contains two *trans*-proline residues (*7*). One of these, Pro140, is near the C-terminus of the domain and may play no significant role in its refolding. The other proline, Pro134, forms part of the peptide binding surface and directly contacts the fluorescent residue Trp119 (Figure 4). Previous studies of proline *cis*−*trans* isomer ratios suggest that 10−30% of unfolded Fyn-SH3 molecules could contain an incorrect, *cis*-proline residue at this position and thus fold with the slow rate (0.1−0.01 $s^{-1}$ at 20 °C) associated with *cis*−*trans* isomerization (*19*). However, native levels both of fluorescence (97 ± 3%) and

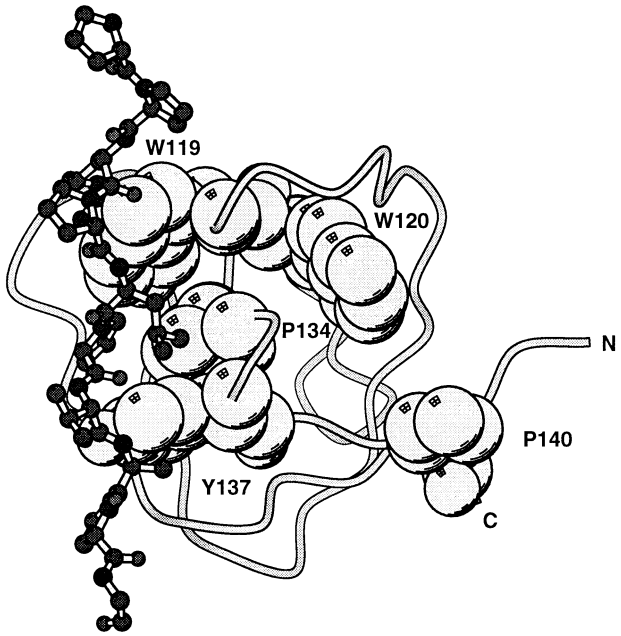


FIGURE 4: Diagrammatic representation of the Fyn-SH3-peptide complex. The peptide is shown in ball-and-stick representation, while the protein is shown as a backbone worm. The program Molscript was used to produce this figure (*18*). Certain Fyn-SH3 residues involved in the interaction are shown in CPK and labeled: the two tryptophan residues, the two proline residues, and tyrosine 137. The structure of Pro134 is clearly constrained by Trp119 and Tyr137, and this observation, together with molecular dynamics simulations (D. Pugh, personal communication), strongly suggests that a *cis*-proline cannot be accommodated at this position without significantly disrupting both the peptide binding surface and the intrinsic fluorescence of the protein.

of peptide binding (95 ± 6%) activity are recovered within 200 ms in 0.727 M GuHCl (Figure 2A,B), and no slow phase ($k$ = 0.02−10 $s^{-1}$) is observed with an amplitude of >2% by fluorescence (data not shown) or >8% by NMR spectroscopy (Figure 2C).

The isomerization of proline residues in near-native folding intermediates has been observed during the refolding of several proteins (e.g., refs *20, 21*). Inspection of the Fyn-SH3 structure suggests, however, that due to the role Pro134 plays in peptide binding and in defining the geometry of the two tryptophan residues, the protein is unlikely to fold to a structure exhibiting the observed native fluorescence and activity if this residue is in the incorrect, *cis*, conformation (Figure 4). Simulated annealing calculations (XPLOR, ref *22*) of the Fyn-SH3 structure with Pro134 restricted to the *cis* conformation produce a highly strained structure with a significantly altered hydrophobic core and binding pocket geometry (D. Pugh and I. D. Campbell, personal communication). This further suggests that it is improbable that a *cis*-proline could be incorporated at this point in the folded protein without significantly disrupting native fluorescence and peptide binding activity.

Traditional methods of monitoring denaturation suggest that in 8 M GuHCl the Fyn-SH3 domain is fully unfolded. Indeed, equilibrium unfolding of the Fyn-SH3 domain indicates that the protein is denatured even at a substantially lower concentration of GuHCl than the 8 M GuHCl used in the above refolding studies (Figure 1). To characterize the 8 M GuHCl denatured state of Fyn-SH3, $^1H-^{13}C$ and $^1H-^{15}N$ HSQC spectra were recorded on isotopically labeled

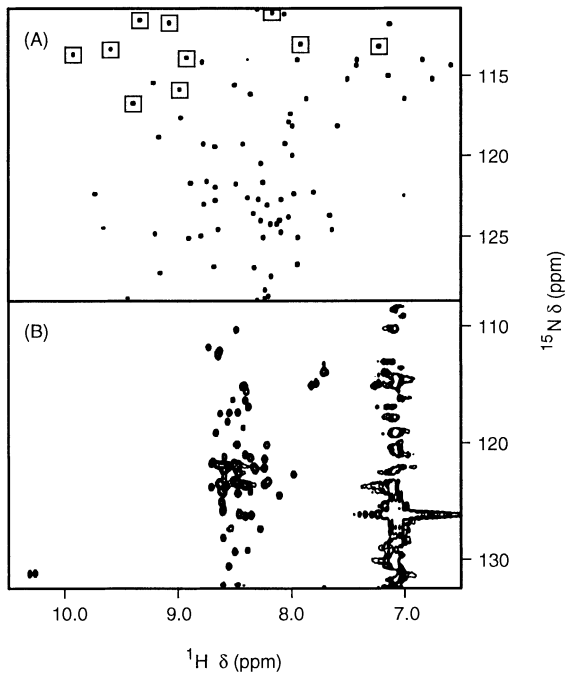


FIGURE 5: $^{1}$H−$^{15}$N HSQC spectra of Fyn-SH3 (A) in 20 mM Tris-HCl, pH 7.2 (Tris), and (B) in 8 M GuHCl/Tris. The signals in boxed regions in (A) are folded signals as a relatively small spectral width was used in the $^{15}$N dimension to improve the resolution of the spectrum. The poor dispersion observed in 8 M GuHCl indicates that the protein is unfolded under these conditions.

samples. Comparison to the spectra of native Fyn-SH3 indicates that there is a substantial loss in dispersion of the amide resonances in denatured Fyn-SH3, consistent with the loss of secondary and tertiary structure (Figure 5). Similarly, the $^{1}$H−$^{13}$C HSQC shows a reduction in dispersion of peaks, particularly of the CαH resonances (data not shown). Of particular interest in the $^{1}$H−$^{13}$C HSQC are the proton resonances of the two proline residues. Both proline Hδ$^{13}$C resonances are shifted from their native chemical shift values of 2.98 and 3.25 ppm (C.J.M. and I.D.C., unpublished data) to 3.79 and 3.86 ppm, which are very close to the values predicted for a random-coil conformation in 8 M GuHCl (3.67 and 3.72 ppm) (*23*). This suggests that the proline-containing sequence is unfolded in 8 M GuHCl.

There are significant differences in the non-C$\delta$ $^{13}$C chemical shift between the *cis*- and *trans*-proline isomers (*24*) which, in principle, should allow the determination of the relative amounts of the two species. In denatured samples of $^{13}$C-labeled Fyn-SH3, spectral overlap renders such an analysis extremely difficult. A small peptide corresponding to the region around Pro134 was, however, more amenable to analysis. A pentapeptide covering residues 132−136 (YIPSN) of the Fyn-SH3 domain was synthesized and studied by 1D $^{1}$H NMR in 8 M GuHCl. The percentage of *cis*-proline in this peptide, as measured by the ratio of peak integrals for the *cis* and *trans* resonances in 1D spectra, was found to be 8 ± 2%. This amount of *cis*-proline in the intact Fyn-SH3 domain should give rise to an observable slow phase during Fyn-SH3 refolding. To clarify the origins of this discrepancy, a peptide corresponding to the 40 carboxy-terminal residues (residues 114−154) of Fyn-SH3 was synthesized with a [$^{13}$C]proline residue included at position 134. The observed chemical shifts (Figure 6) are

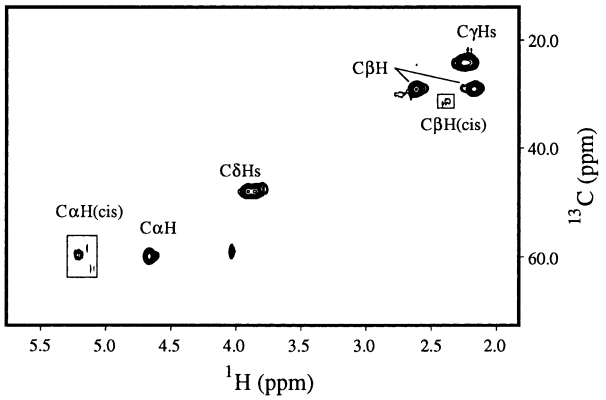


FIGURE 6: $^{1}$H−$^{13}$C HSQC of a synthetic peptide in 8 M GuHCl. The sequence of the peptide corresponds to the 40 C-terminal residues of Fyn-SH3 and contains $^{13}$C-proline at the position of residue Pro134. The *trans*-proline peaks are all shown and labeled. The well-resolved cross-peaks from *cis*-proline resonances are shown in boxed regions at a threshold level 1/4 that of the rest of the spectrum. Resonances from the *cis*-proline (4 ± 2% of the *trans* peak volumes) are substantially weaker than those arising from the *trans* conformer, indicating an unusually low *cis*−*trans* ratio.

consistent with those expected for a random-coil conformation in 8 M GuHCl (*23*). Analysis of $^{1}$H−$^{13}$C HSQC spectra of this construct indicated that the level of *cis* Pro134 in 8 M GuHCl was, however, only 4 ± 2%. If the actual ratio falls within the lower half of the confidence range, or the isomerization rate is very slow (<0.02 s$^{-1}$), then it would not give rise to an observable phase in the folding experiments monitored by fluorescence due to sample diffusion, lamp drift, and photobleaching. This may be the reason for the lack of an observable proline isomerization limited refolding phase.

Protein folding does not obey simple Arrhenius kinetics due, at least in part, to the influence of a relatively large difference in the heat capacities of the transition and denatured states ($\Delta C_p^{\ddagger}$) (*25, 26*). The contribution of $\Delta C_p^{\ddagger}$ to the temperature dependence of the folding rate is often described by a modification of the Eyring equation (*25*). For a two-state folding transition, the modified equation is

$$\ln (k_f/T) = \ln (k_b/h) + [\Delta S^{\ddagger}(T_0) - \Delta H^{\ddagger}(T_0)/T]/R + \Delta C_p^{\ddagger} [\ln (T/T_0) + T_0/T - 1]/R$$

where $T$ is the absolute temperature; $k_b$, $h$, and $R$ are respectively the Boltzmann, Planck, and gas constants; and $\Delta H^{\ddagger}(T_0)$ and $\Delta S^{\ddagger}(T_0)$ are the values of the activation enthalpy and entropy of folding, respectively, at an arbitrary reference temperature $T_0$. The term $k_b/h$, originating from the preexponential probability term in the Eyring equation, represents the probability of a molecule with as much or more energy than the transition barrier actually passing over the barrier, while the remainder of the equation calculates a pseudoequilibrium between the starting state and conformations higher in energy than the barrier. Figure 7 shows an Eyring plot [ln ($k_f/T$) versus 1/$T$] for the refolding rate of Fyn-SH3 against temperature. The data are well fit to the above equation ($r^2$ = 0.9996) with the following relative thermodynamic parameters: $\Delta H^{\ddagger}$(293 K) = 10.3 ± 0.01 kcal mol$^{-1}$, $\Delta S^{\ddagger}$(293 K) = −0.0172 ± 0.0003 kcal mol$^{-1}$ K$^{-1}$, and $\Delta C_p^{\ddagger}$ = −0.444 ± 0.006 kcal mol$^{-1}$ K$^{-1}$.

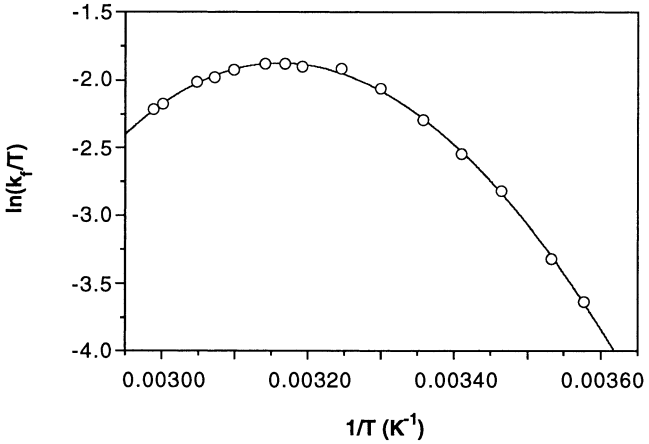


FIGURE 7: Eyring plot [ln ($k$/$T$) versus 1/$T$] for the temperature dependence of Fyn-SH3 refolding over the range 6−60 °C (the $T_m$ of Fyn-SH3 is 72 °C; ref *32*). The fit indicates a $\Delta C_p^{\ddagger}$ of −0.444 kcal mol$^{-1}$ K$^{-1}$, which is about half that of the native protein (−0.86 kcal mol$^{-1}$ K$^{-1}$; ref *32*). Since $\Delta C_p$ is known to correlate with the relative solvent-accessible surface area (ref *17*, and references cited therein), this might indicate that the transition state of folding is only moderately collapsed. Analysis of the ratio $\alpha = m^{\ddagger}_f/(m^{\ddagger}_u - m^{\ddagger}_f)$, also thought to reflect the relative solvent-accessible surface area of the transition state, is significantly higher (Figure 3). The origins of this discrepancy are unclear, but a similar discrepancy appears in data from several other two-state proteins (see Conclusions).

## CONCLUSIONS

The kinetics and thermodynamics of folding of the Fyn-SH3 domain fit well to a two-state model. The equilibrium data indicate that the protein undergoes effectively a single transition between a native and denatured conformation, with no significant intermediates populated under equilibrium conditions. Kinetic analysis is perhaps more sensitive to the appearance of folding intermediates than is equilibrium denaturation, but the kinetic data for Fyn-SH3 are also well fitted by a two-state folding model. Consistent with the apparently two-state refolding of Fyn-SH3, the refolding kinetics of the domain are monophasic and effectively identical, whether probed by intrinsic fluorescence or by the recovery of peptide binding activity. This suggests that species with a fluorescence differing from that of the native or unfolded states do not accumulate during the folding process. A plot of ln ($k$) versus [GuHCl] is linear in the extremes of high and low denaturant concentration, further suggesting that no stable intermediates are populated during refolding. Last, the values of $\Delta G_{H_2O}$ and $m_{eq}$ are very similar whether calculated from equilibrium or kinetic data. While values for $\Delta G_{H_2O}$ are within experimental error, the values for $m_{eq}$ differ by slightly more than the experimental error. This disparity may be a result of the difficulty in analysis of the equilibrium data, due to the significant dependencies of both native and denatured Fyn-SH3 fluorescence on the concentration of GuHCl (*2*). The refolding kinetics of the spectrin (*2*), src (*4*), and PI3 SH3 domains (*5*) are also well fitted by a two-state model.

There is no indication of a proline isomerization-limited refolding phase in Fyn-SH3, despite the presence of a proline residue in the ligand binding site and the absolute requirement for the *trans* isomer at this residue to form the native structure. While this may be due to a large increase in the rate of proline isomerization during the folding process (*27*), it is possible that it is simply the result of an unusually small population of the *cis* isomer in the unfolded protein. The *cis*−*trans* ratio, 4 ± 2%, is substantially smaller than the 10−33% ratios previously reported for small peptides or unfolded proteins (*28*) but is similar in magnitude to the proline isomerization linked event reported during the refolding of the SH3 domain from spectrin (*2*). The basis for such a low *cis*−*trans* ratio is unclear. Under identical conditions, a synthetic pentapeptide corresponding to the sequence around Pro134 of Fyn-SH3 shows a *cis*−*trans* proline ratio of 8 ± 2%. While these values overlap with that for the protein, they suggest that nonlocal sequence effects may result in a slightly lower level of *cis* isomer in the denatured protein. This is highlighted by the 10% proline isomerization-limited phase observed for the src SH3 domain (*4*) which has an identical sequence around the equivalent proline residue. The evidence for any residual structure in denatured Fyn-SH3, however, is lacking and at this stage, our data are unable to support a definitive statement as to the reason for the lack of observable proline isomerization during refolding. This is a question worthy of further investigation, as several other proline-containing proteins appear to lack isomerization-like folding phases (e.g., refs *29, 30*) including the relatively stable, tenth fibronectin type III domain of human fibronectin which contains eight proline residues (*31*).

Equilibrium studies of protein folding suggest that both the temperature and denaturant dependence of protein folding kinetics can provide a means of monitoring the conformation of the transition state. The folding transition state $m$-value of Fyn-SH3 is 68% that of the native protein, suggesting that the transition state is a relatively compact structure. The transition state heat capacity ($\Delta C_p^{\ddagger}$) is −0.444 kcal mol$^{-1}$ K$^{-1}$, which is only 51% that of the native protein (*32*). As equilibrium studies suggest that both $m$ and $\Delta C_p$ are directly proportional to changes in the relative solvent-accessible surface area (*17*), this discrepancy is somewhat surprising. However, a similar discrepancy appears for all of the single-domain proteins for which we have data, including the *Bacillus* cold shock protein (*29, 33*), chymotrypsin inhibitor-2 (*34*), protein L (*26*), the bacterial phosphotransferase protein HPr (*35*), and human acyl phosphatase (F. Chiti, personal communication). Possible origins for this discrepancy include the inappropriateness of using an Eyring equation-type model, derived to describe gas-phase reactions, to fit data derived from a complex, condensed-phase protein folding reaction (*36*), or because of temperature-induced changes in the folding transition state.

Homology studies provide an opportunity to study the role of global properties, such as stability and gross sequence composition, in defining the kinetics of protein folding in the absence of such complicating factors as significantly differing topologies. The results presented in this paper for Fyn-SH3, when taken with the results for the SH3 domains of spectrin (*2, 10, 37*), drk (*6*), src (*3, 4*) and PI3 (*5*), represent the largest study to date of the refolding of members of a family of homologous proteins (see ref *38* and references cited therein). We have used this data set to investigate the transition state placement and the importance of equilibrium stability and relative sequence identity in defining the relative folding rates of homologous proteins

```
Fyn    TLFVALYDYEARTEDDLSFHKGEKFQI        LNSSEGD        WWEARSLTTGETGYIPSNYVAPVD
src    TTFVALYDYESRTETDLSFKKGERLQI        VNNTEGD        WWLAHSLTTGQTGYIPSNYVAPSD
spec   ELVLALYDYQEKSPREVTMKKGDILTL        LNSTNKD        WWKVE  VNDRQGFVPAAYVKKLD
drk    MEAIAKHDFSATADDELSFRKTQILKI        LNMEDDSN       WYRAE  LDGKEGLIPSNYIEMKN
PI3    YQYRALYDYKKEREEDIDLHLGDILTVNKGSLVALGFSDGQEAKPEEIGWLNGYNETTGERGDFPGTYVEYIG
```

FIGURE 8: Sequence alignment of the SH3 domains from Fyn, src, spectrin, drk, and PI3. The conserved residues relative to Fyn-SH3 are underlined. Most of the conserved residues in SH3 domains are surface-exposed and are involved in the peptide binding site rather than in the hydrophobic core of the corresponding protein (*41*, *43*, *39*, *47*). Despite this fact, and the often low sequence identity among SH3 domains, these show a common core structure.

Table 1: Sequence Identity and Thermodynamic and Kinetic Parameters for Five SH3 Domains [a]

| | src (%) | spectrin (%) | drk (%) | PI3 (%) | α (%) | $\Delta G_{H_2O}$ (kcal mol$^{-1}$) | $k_{f-H_2O}$ (s$^{-1}$) | $m_{eq}$ (kcal mol$^{-1}$ M$^{-1}$) | $m^{\ddagger}_f$ (M$^{-1}$) |
|---|---|---|---|---|---|---|---|---|---|
| Fyn | 78 | 34 | 35 | 36 | 0.68 | −6.0 | 94.0 | −1.4 | −1.9 |
| src | | 34 | 32 | 31 | 0.69 | −4.1 | 56.7 | −1.4 | −1.7 |
| spectrin | | | 23 | 29 | 0.69 | −3.8 | 4.0 | −0.7 | −0.9 |
| drk | | | | 23 | NA | ∼0 | 0.9 | NA | NA |
| PI3 | | | | | 0.60 | −3.4 | 0.35 | −2.3 | −2.4 |

[a] Pairwise identities were calculated with the program AMPS (*14*) based on the sequence alignment shown in Figure 8. Thermodynamic and kinetic data are taken from the literature as follows: src, ref (*4*); spectrin, refs (*10*, *37*); drk, ref (*6*); PI3−SH3, ref (*5*). NA: data are not available. Temperatures used to obtain these data in the corresponding studies are as follows: Fyn-SH3, 20 °C; src, 22 °C; spectrin, 25 °C; PI3-SH3, 20 °C; drk, 14 °C. Note that $m^{\ddagger}_f$ is expressed in M$^{-1}$ units.

sharing a similar structure. The structures of the SH3 domains from Fyn (*7*, *39*), src (*40*), spectrin (*41*, *42*), and PI3 (*43*, *44*, *45*) have been solved by either NMR, X-ray crystallography, or both, and a homology-based model has been proposed for drk (*6*, *46*). These domains have a common global core structure. For instance, the atomic root-mean-square deviation (RMSD) of the structure superposition of PI3 and src SH3 domains over 21 residues found in regions of conserved $\beta$-sheet is only 0.81 Å (*43*), while the RMSD of the superposition of Fyn-SH3 and spectrin structures over 51 Cα atoms is 1.1 Å (*39*). Despite sharing a common topology, however, the SH3 domains often display a very low sequence identity (Figure 8 and Table 1).

The ratio $\alpha = m^{\ddagger}_f/(m^{\ddagger}_u - m^{\ddagger}_f)$ is thought to reflect the solvent-exposed hydrophobic surface area of the transition state (or ensemble of states) relative to the native state. Hence, it is thought to represent the placement of the transition state on a reaction coordinate defined by the degree of collapse of the polypeptide chain. For Fyn-SH3, this value is 0.68, suggesting that the transition state is relatively compact and nativelike. Effectively identical values of α have been observed for the spectrin (0.69, ref *37*) and src (0.69, ref *4*) SH3 domains. This might arise if the conformation of the structured residues in the transition states of these proteins is, like their native structures, conserved despite the relatively low pairwise sequence identities (Table 1) (*48*). Furthermore, if key aspects of the folding nucleus are conserved, then a homologous SH3 domain containing additional residues not present in the nucleus would exhibit a lower α ratio because a smaller fraction of its polypeptide chain would be structured in the transition state. This may account for the lower α ratio observed for the PI3-SH3 domain (0.60, ref *5*), which contains an approximately 15 residue loop not present in the other SH3 domains; it is noteworthy that long loops such as this are known to remain unstructured in the transitions states of barnase and the chymotrypsin inhibitor-2 (*49*, *50*). Similar conservation of α has been observed between other sets of homologous proteins (*51*, *52*, *38*), suggesting that the gross structural features of their folding transition states are also conserved.

To analyze the role of thermodynamic stability in defining the folding rate of homologous proteins it is important that these fold in a process lacking significantly populated intermediates, as the formation of an intermediate could be rate-limiting, and thereby complicate the analysis. Fortunately, the SH3 domains studied so far fold without effective accumulation of intermediates and can thus be used for such analysis. Theoretical (*53*, *54*, *55*, *56*) and limited experimental (*38*, *52*) evidence has suggested that the folding rates of homologous proteins which fold via a two-state mechanism may parallel their thermodynamic stability. In accord with this hypothesis, under similar conditions (i.e., no denaturant, similar temperature), the more stable Fyn refolds approximately 2, 24, 105, and 270 times faster than the src, spectrin, drk, and PI3 SH3 domains, respectively (see Table 1). When the folding rates of the SH3 domains for which data are available are compared over a large range of denaturant concentration, rates differing by as much as 3 orders of magnitude can be observed (Figure 9A). However, under conditions of equal stability, the refolding rates of the SH3 domains of Fyn, spectrin, and PI3 are rather similar over a wide range of denaturant concentration (Figure 9B). For instance, in the presence of sufficient denaturant to reduce the stability of Fyn-SH3 to −3.4 kcal mol$^{-1}$ (the free energy of unfolding of PI3-SH3 at 20 °C in the absence of denaturant), its folding rate is only ∼3- and ∼8-fold faster than the folding rate of the spectrin and PI3 SH3 domains, respectively (instead of ∼24- and ∼270-fold faster at zero denaturant concentration). These data suggest that thermodynamic stability is an important factor in determining the relative folding rates of homologous proteins.

Among the characterized SH3 domains, Fyn and src are the most closely related, with a sequence identity of 78% (Table 1). It is therefore particularly interesting that in contrast to the situation discussed above for the other SH3 domains (which only show pairwise identities of 36% or lower), the folding rates of Fyn and src SH3 domains are actually closer to each other at the same denaturant concen-

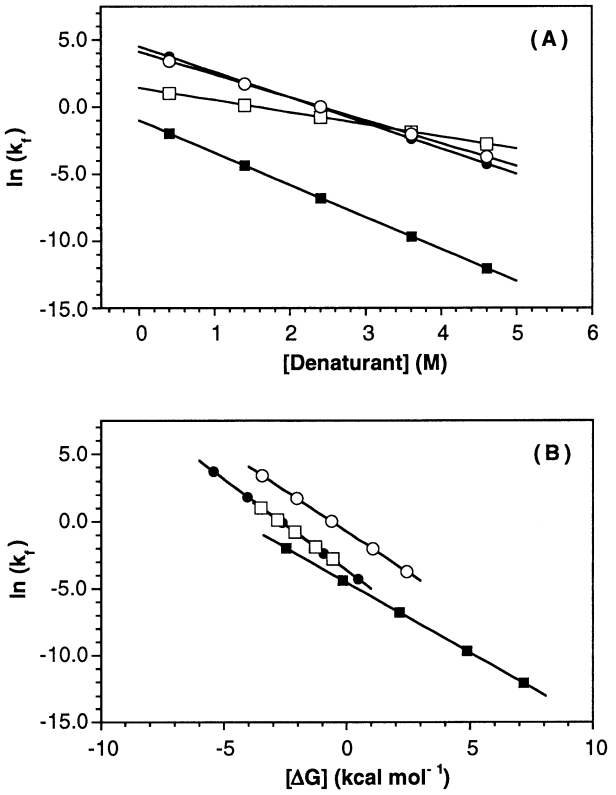


FIGURE 9: Logarithm of the refolding rate [ln ($k_f$)] as a function of (A) denaturant concentration and (B) the equilibrium free energy of folding ($\Delta G$). (●) Fyn-SH3; (○) src SH3; (□) spectrin SH3; (■) PI3-SH3. Lines are idealized curves calculated using the thermodynamic and kinetic data shown in Table 1 and the following equations: $\ln(k_f) = \ln(k_{f-H_2O}) + m^{\ddagger}_f$[denaturant]; and $\Delta G = \Delta G_{H_2O} - m_{eq}$[denaturant]. These equations describe the linear dependence of ln ($k_f$) and $\Delta G$ on denaturant concentration, respectively. Symbols do not represent experimental data. Note that the slope ($m^{\ddagger}_f$) of the curve corresponding to spectrin SH3 in (A) is about 2-fold smaller than that of the other SH3 domains. This is due to the fact that experiments with spectrin were performed using urea as denaturant while GuHCl was employed for the other proteins, and *m* values are generally smaller in urea by a factor of 2 (*17*). At the same final denaturant concentration, the refolding rates of the SH3 domains can differ by as much as 3 orders of magnitude. However, with the exception of the src SH3, under denaturant conditions producing equal stability (same $\Delta G$) the refolding rates of the SH3 domains are within a factor of 10.

tration than at the same free energy of folding (see Figure 9). One possible explanation of this observation is that one or more of the sequence changes unique to src SH3 result in a destabilization of the native structure but not of the transition state. Such a situation would most simply arise if the residue or residues involved were to be located in a region of the protein that is not highly structured in the transition state. Whether or not this explanation is correct cannot, however, be deduced from the available data. Indeed, no relationship is evident between the sequence identities of the presently characterized SH3 domains and their stabilities, folding kinetics, or characteristics ($\alpha$ values) of their transition states (see Table 1). Nevertheless, this finding, along with earlier observations [e.g., that the least stable of two homologous forms of the IgG binding domain of streptococcal protein G folds more rapidly (*57*)], suggests that specific sequence details, in addition to thermodynamic stability, can play a significant role in defining the relative refolding rates of natural proteins sharing a given topology.

## ACKNOWLEDGMENTS

We thank David Pugh, Viara Grantcharova, David Baker, David Riddle, Michelle Scalley, Nico van Nuland, and Fabrizio Chiti for communicating important prepublication results. We also thank Chris Rudd for providing the Fyn-SH3−GST fusion clones and Dennis Benjamin for conducting Fyn-SH3 mass spectrometric analyses.

## REFERENCES

1. Morton, C. J., and Campbell, I. D. (1994) *Curr. Biol. 4*, 615−617.
2. Viguera, A. R., Martínez, J. C., Filimonov, V. V., Mateo, P. L., and Serrano, L. (1994) *Biochemistry 33*, 2142−2150.
3. Riddle, D. S., Santiago, J. V., Bray-Hall, S. T., Doshi, N., Grantcharova, V. P., Yi, Q., and Baker, D. (1997) *Nat. Struct. Biol. 4*, 805−809.
4. Grantcharova, V. P., and Baker, D. (1997) *Biochemistry 36*, 15685−15692.
5. Guijarro, J. I., Morton, C. J., Plaxco, K. W., Pitkeathly, M., Campbell, I. D., and Dobson, C. M. (1998) *J. Mol. Biol.* (in press).
6. Farrow, N. A., Zhang, O., Forman-Kay, J. D., and Kay, L. E. (1995) *Biochemistry 34*, 868−878.
7. Morton, C. J., Pugh, D. J. R., Brown, E. L. J., Kahmann, J. D., Renzoni, D. A. C., and Campbell, I. D. (1996) *Structure 4*, 705−714.
8. Renzoni, D. A. C., Pugh, D. J. R., Siligardi, P. D., Morton, C. J., Rossi, C., Waterfield, M. D., Campbell, I. D., and Ladbury, J. E. (1996) *Biochemistry 35*, 15646−15653.
9. Nozaki, Y. (1972) *Methods Enzymol. 26*, 43−51.
10. Viguera, A. R., Blanco, F. J., and Serrano, L. (1995) *J. Mol. Biol. 247*, 670−681.
11. Balbach, J., Forge, V., van Nuland, N. A. J., Winder, S. L., Hore, P. J., and Dobson, C. M. (1995) *Nat. Struct. Biol. 2*, 865−870.
12. Bruhwiler, D., and Wagner, G. (1986) *J. Magn. Reson. 69*, 546−551.
13. Kay, L. E., Keifer, P., and Saarinen, T. (1992) *J. Am. Chem. Soc 114*, 10663−10665.
14. Barton, G. J. (1990) *Methods Enzymol. 183*, 403−428.
15. Khorasanizadeh, S., Peters, I. D., Butt, T. R., and Roder, H. (1993) *Biochemistry 32*, 7054−7063.
16. Jackson, S. E., and Fersht, A. R. (1991) *Biochemistry 30*, 10428−10435.
17. Myers, J. K., Pace, N., and Scholtz, J. M. (1995) *Protein Sci. 4*, 2138−2148.
18. Kraulis, P. J. (1991) *J. Appl. Crystallogr. 24*, 946−950.
19. Creighton, T. E. (1978) *J. Mol. Biol. 125*, 401−406.
20. Schmid, F. X., and Blaschek, H. (1981) *Eur. J. Biochem. 114*, 111−117.
21. Evans, P. A., Kautz, R. A., Fox, R. O., and Dobson, C. M. (1989) *Biochemistry 28*, 362−370.
22. Brünger, A. T. (1992) *X-PLOR version 3.1. A system for X-ray crystallography and NMR*, Yale University Press, New Haven, CT.
23. Plaxco, K. W., Morton, C. J., Grimshaw, S. B., Jones, J. A., Pitkeathly, M., Campbell, I. D., and Dobson, C. M. (1997) *J. Biomol. NMR 10*, 221−230.
24. Howarth, O. W., and Lilley, D. M. J. (1978) *Prog. NMR Spectrosc. 12*, 1−40.
25. Jackson, S. E., and Fersht, A. R. (1991) *Biochemistry 30*, 10436−10443.
26. Scalley, M. L., and Baker, D. (1997) *Proc. Natl. Acad. Sci. U.S.A. 94*, 10636−10640.
27. Cook, K. H., Schmid, F. X., and Baldwin, R. L. (1979) *Proc. Natl. Acad. Sci. U.S.A. 76*, 6157−6161.
28. Dyson, H. J., and Wright, P. E. (1991) *Annu. Rev. Biophys. Biophys. Chem. 20*, 519−538.
29. Schindler, T., Herrler, M., Marahiel, M. A., and Schmid, F. X. (1995) *Nat. Struct. Biol. 2*, 663−673.
30. Kragelund, B. B., Robinson, C. V., Knudsen, J., Dobson, C. M., and Poulsen, F. M. (1995) *Biochemistry 34*, 7217−7224.

31. Plaxco, K. W., Spitzfaden, C., Campbell, I. D., and Dobson, C. M. (1996) *Proc. Natl. Acad. Sci. U.S.A. 93*, 10703−10706.
32. Azuaga, A. I. (1995) Doctoral Thesis, p 212, University of Granada, Granada, Spain.
33. Schindler, T., and Schmid, F. X. (1996) *Biochemistry 35*, 16833−16842.
34. Tan, Y.-J., Oliveberg, M., and Fersht, A. R. (1996) *J. Mol. Biol. 264*, 377−389.
35. van Nuland, N. A. J., Meijberg, W., Warner, J., Forge, V., Scheek, R. M., Robillard, G. T., and Dobson, C. M. (1998) *Biochemistry* (in press).
36. Dill, K. A., and Chan, H. S. (1997) *Nat. Struct. Biol. 4*, 10−19.
37. Viguera, A. R., Serrano, L., and Wilmanns, M. (1996) *Nat. Struct. Biol. 3*, 874−880.
38. Plaxco, K. W., Spitzfaden, C., Campbell, I. D., and Dobson, C. M. (1997) *J. Mol. Biol. 270*, 763−770.
39. Noble, M. E. M., Musacchio, A., Saraste, M., Courtneidge, S., and Wierenga, R. K. (1993) *EMBO J. 12*, 2617−2624.
40. Yu, H., Rosen, M. K., Shin, T. B., Seidel-Dugan, C., Brugge, J. S., and Schreiber, S. L. (1992) *Science 258*, 1665−1668.
41. Musacchio, A., Noble, M. E. M., Pauptit, R., Wierenga, R. K., and Saraste, M. (1992) *Nature 359*, 851−855.
42. Blanco, F. J., Ortiz, A. R., and Serrano, L. (1997) *J. Biomol. NMR 9*, 347−357.
43. Booker, G. W., Gout, I., Downing, A. K., Driscoll, P. C., Boyd, J., Waterfield, M. D., and Campbell, I. D. (1993) *Cell 73*, 813−822.
44. Koyama, S., Yu, H., Dalgarno, D. C., Shin, T. B., Zydowsky, L. D., and Schreiber, S. L. (1993) *Cell 72*, 945−952.
45. Liang, J., Chen, J. K., Schreiber, S. L., and Clardy, J. (1996) *J. Mol. Biol. 257*, 632−643.
46. Zhang, O., and Forman-Kay, J. D. (1995) *Biochemistry 34*, 6784−6794.
47. Musacchio, A., Willmanns, M., and Saraste, M. (1994) *Prog. Biophys. Mol. Biol. 61*, 283−297.
48. Shakhnovich, E. I., Abkevich, V., and Ptitsyn, O. B. (1996) *Nature 379*, 96−98.
49. Fersht, A. R., Bycroft, M., Horovitz, A., Kellis, J. T., Matouschek, A., and Serrano, L. (1991) *Philos. Trans. R. Soc. London 332*, 171−176.
50. Itzhaki, L. S., Otzen, D. E., and Fersht, A. R. (1995) *J. Mol. Biol. 254*, 260−288.
51. Kragelund, B. B., Højrup, P., Jensen, M. S., Schjerling, C. K., Juul, E., Knudsen, J., and Poulsen, F. M. (1996) *J. Mol. Biol. 256*, 187−200.
52. Mines, G. A., Pascher, T., Torbjorn, P., Lee, S. C., Winkler, J. R., and Gray, H. B. (1996) *Chem. Biol. 3*, 491−497.
53. Finkelstein, A. V. (1991) *Proteins Struct., Funct., Genet. 9*, 23−27.
54. Sali, A., Shakhnovich, E., and Karplus, M. (1994) *Nature 369*, 248−251.
55. Bryngelson, J. D., Onuchic, J. N., Socci, N., and Wolynes, P. G. (1995) *Proteins: Struct., Funct., Genet. 21*, 167−195.
56. Onuchic, J. N., Wolynes, P. G., Luthey-Schulten, Z., and Socci, N. (1995) *Proc. Natl. Acad. Sci. U.S.A. 92*, 3626−3630.
57. Alexander, P., Orban, J., and Bryan, F. (1992) *Biochemistry 31*, 7243−7248.

BI972075U